JOC Article
pubs.acs.org/joc

Polyaza Cryptand Receptor Selective for Dihydrogen Phosphate

Pedro Mateus,[†] Rita Delgado,*[,†,‡] Paula Brandão,[§] and Vítor Félix[∥]

[†]*Instituto de Tecnologia Química e Biológica, UNL, Av. da República-EAN, 2780-157 Oeiras, Portugal,* [‡]*Instituto Superior Técnico, DEQB, Av. Rovisco Pais, 1049-001 Lisboa, Portugal,* [§]*Departamento de Química, CICECO, Universidade de Aveiro, 3810-193 Aveiro, Portugal, and* [∥]*Departamento de Química, CICECO, and Secção Autónoma de Ciências da Saúde, Universidade de Aveiro, 3810-193 Aveiro, Portugal*

delgado@itqb.unl.pt

Received August 11, 2009

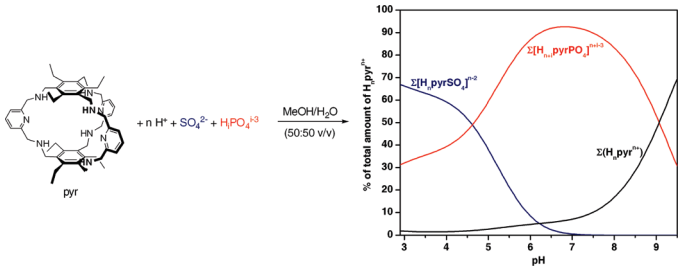

A hexaamine cage with pyridyl spacers was synthesized in good yield by a [2+3] Schiff-base condensation followed by sodium borohydride reduction. The protonation constants of the receptor as well as its association constants with Cl^-, NO_3^-, AcO^-, ClO_4^-, SO_4^{2-}, $H_2PO_4^-$, and $H_2AsO_4^-$ were determined by potentiometry at 298.2 ± 0.1 K in H_2O/MeOH (50:50 v/v) and at ionic strength 0.10 ± 0.01 M in KTsO. These studies revealed that although dihydrogen phosphate is less charged than sulfate, it is still appreciably bound by the receptor at low pH, suggesting that the pyridyl nitrogen is accepting hydrogen bonds from dihydrogen phosphate. It is also shown that dihydrogen phosphate is capable of effectively competing with sulfate for the receptor at higher pH, being selective for hydrogen phosphate at pH about 7.0. ^{31}P NMR experiments supported these findings. The fact that the receptor shows such a marked preference for hydrogen phosphate based mainly in its hydrogen bond accepting/donating ability in a highly competitive medium such as water/methanol mixed solvent is quite remarkable. Single-crystal X-ray diffraction determinations of anion associations between H_6pyr^{6+} receptor and nitrate, sulfate, and phosphate are consistent with the existence of $[(H_6pyr)(NO_3)_3(H_2O)_3]^{3+}$, $[(H_6pyr)(SO_4)_2(H_2O)_4]^{2+}$, and $[(H_6pyr)(HPO_4)_2(H_2PO_4)(H_2O)_2]^+$ cations. One nitrate anion is embedded into the H_6pyr^{6+} cage of the first supermolecule whereas in the second and third ones the anions are located in the periphery of the macrobicycle.

Introduction

The important role played by anions in environmental and natural processes has triggered the interest in the development of synthetic receptor molecules for their selective recognition and transport. Among anionic substrates, phosphate and sulfate are of special interest due to their ubiquitous presence in biological systems and also because of their well-known deleterious effects on the environment.[1]

In Nature, the sulfate-binding protein (SBP) and the phosphate-binding protein (PBP) take advantage of the backbone amide NH groups to tightly bind their respective substrates with a network of several hydrogen bonds in the interior of a deep cleft completely inaccessible to the solvent.[2,3] The most striking difference between these two proteins is the presence of the carboxylate group of an aspartate residue that functions as a hydrogen bond acceptor

*To whom correspondence should be addressed. Phone: (+351) 21 446 9737. Fax: (+351) 21 441 1277.

(1) Bianchi, A.; Bowman-James, K.; Garcia-España, E.; *Supramolecular Chemistry of Anions*; Wiley-VCH: New York, 1997. Steed, J. W.; Atwood, J. L.; *Supramolecular Chemistry*, 2nd ed.; John Wiley & Sons, Ltd: Hoboken, NJ, 2009.

(2) Pflugrath, J. W.; Quiocho, F. A. *Nature* **1985**, *314*, 257.
(3) Luecke, H.; Quiocho, F. A. *Nature* **1990**, *347*, 402.

Published on Web 10/27/2009 DOI: 10.1021/jo901742d

CHART 1. Polyaza Cryptands Discussed in This Work

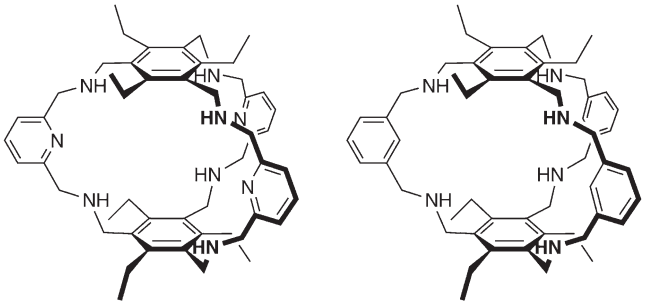

for the phosphate OH in PBP. This feature allows PBP to discriminate phosphate from other similar tetrahedral oxyanions such as sulfate, which in normal pH lacks OH groups and additionally is repelled by the carboxylate negative charge. Conversely SBP has no hydrogen bond acceptors making it unsuitable for protonated oxyanions.[4]

Polyamines are one of the most successful groups of compounds used as receptors for the binding of anions in aqueous medium, due to the versatile nature of the amino group.[5] Amines can be protonated to provide the necessary positive charge to interact with anions and to impart water solubility. The amino group can also act as hydrogen bond donor and as hydrogen bond acceptor if not protonated, which may be useful for the binding of protonated anions such as phosphates. Indeed, several examples of phosphate binding by polyammonium receptors have been reported.[6]

Early on we synthesized a 2,4,6-triethylbenzene capped polyamine cryptand with *m*-xylyl spacers (xyl, Chart 1) which in its protonated forms showed remarkable affinity and selectivity for tetrahedral dianionic species in water/methanol mixed solvent.[7] This study suggested that the discrimination of sulfate from phosphate resulted from the fact that at high degree of protonation the receptor lacks hydrogen bond acceptors for dihydrogen phosphate OH groups, resembling the natural systems. It has been pointed out that the introduction of hydrogen bond acceptors for the OH groups of phosphate into an anion receptor should lead to selective recognition of di- or monohydrogen phosphate.[8]

TABLE 1. Overall (β_i^H) and Stepwise protonation (K_i^H) Constants of pyr in H_2O/MeOH (50:50 v/v) ($T = 298.2 \pm 0.1$ K and $I = 0.10 \pm 0.01$ M in KTsO)

equilibrium	log β_i^H [a]	equilibrium	log K_i^H
$pyr + H^+ \rightleftharpoons Hpyr^+$	8.72(1)	$pyr + H^+ \rightleftharpoons Hpyr^+$	8.72
$pyr + 2\,H^+ \rightleftharpoons H_2pyr^{2+}$	16.61(1)	$Hpyr^+ + H^+ \rightleftharpoons H_2pyr^{2+}$	7.89
$pyr + 3\,H^+ \rightleftharpoons H_3pyr^{3+}$	23.76(1)	$H_2pyr^{2+} + H^+ \rightleftharpoons H_3pyr^{3+}$	7.15
$pyr + 4\,H^+ \rightleftharpoons H_4pyr^{4+}$	30.16(1)	$H_3pyr^{3+} + H^+ \rightleftharpoons H_4pyr^{4+}$	6.40
$pyr + 5\,H^+ \rightleftharpoons H_5pyr^{5+}$	35.85(1)	$H_4pyr^{4+} + H^+ \rightleftharpoons H_5pyr^{5+}$	5.70
$pyr + 6\,H^+ \rightleftharpoons H_6pyr^{6+}$	40.39(1)	$H_5pyr^{5+} + H^+ \rightleftharpoons H_6pyr^{6+}$	4.54

[a] Values in parentheses are standard deviations in the last significant figure.

Pyridyl moieties have been used in this regard and selectivity for dihydrogen phosphate was achieved by the hydrogen bond acceptor of the pyridyl group.[9] Bearing this in mind we decided to take advantage of the macrobicyclic architecture used before[7] and incorporate on its framework pyridyl spacers (pyr, Chart 1) in order to have a cavity with hydrogen bond acceptors and evaluate the effect on the selectivity pattern.

Results and Discussion

Synthesis of pyr. The hexaamine cryptand containing pyridyl spacers was prepared by reaction between 1,3,5-tris(aminomethyl)-2,4,6-triethylbenzene and 2,6-pyridinedicarbaldehyde in 2:3 ratio in MeCN, followed by addition of sodium borohydride for the reduction of imines to amines. This compound is the hexaamine version of the polyamide bicyclic cyclophane reported by Anslyn et al. obtained by a [2+3] reaction between 1,3,5-tris(aminomethyl)-2,4,6-triethylbenzene and 2,6-pyridinedicarbonyl chloride.[10] The pyr cryptand was obtained in 55% yield suggesting that the preorganization of caps and spacers is not the only factor controlling the cyclization process.[7] In fact, as in this type of synthesis the reversible imine condensation is driven toward the formation of the [2+3] product by precipitation, the hexaimine being the thermodynamically favored product, it is likely that the solubility of the final product in the solvent used may also affect the yield.

Potentiometric Studies. Acid−Base Behavior. Potassium tosylate was chosen as the electrolyte to maintain the ionic strength as this bulky anion did not appreciably interact with the receptor.[7] The studies were performed in H_2O/MeOH (50:50 v/v) due to the precipitation of the receptor at pH 7.22 in pure water, preventing the determination of the first two protonation constants in that medium, and also to allow direct comparison with the related compound xyl (see Chart 1). The protonation constants of pyr were thus determined at ionic strength 0.10 M in KTsO and at 298.2 K in H_2O/MeOH (50:50 v/v). The results are collected in Table 1.

Six protonation constants were found for pyr in the working pH region (2.9−9.5), corresponding to the successive protonations of the secondary amines. The stepwise values decrease steadily with increasing protonation state

(4) Jacobson, B. L.; Quiocho, F. A. *J. Mol. Biol.* **1988**, *204*, 783.
(5) (a) Ilioudis, C. A.; Steed, J. W. *J. Supramol. Chem.* **2001**, *1*, 165. (b) Llinares, J. M.; Powell, D.; Bowman-James, K. *Coord. Chem. Rev.* **2003**, *240*, 57. (c) García-España, E.; Díaz, P.; Llinares, J. M.; Bianchi, A. *Coord. Chem. Rev.* **2006**, *250*, 2952. (d) McKee, V.; Nelson, J.; Town, R. M. *Chem. Soc. Rev.* **2003**, *32*, 309.
(6) (a) Dietrich, B.; Guilhem, J.; Lehn, J.-M.; Pascard, C.; Sonveaux, E. *Helv. Chim. Acta* **1984**, *67*, 91. (b) Motekaitis, R. J.; Martell, A. E. *Inorg. Chem.* **1992**, *31*, 5534. (c) Nation, D. A.; Reibenspies, J.; Martell, A. E. *Inorg. Chem.* **1996**, *35*, 4597. (d) Lu, Q.; Reibenspies, J. H.; Carroll, R. I.; Martell, A. E.; Clearfiled, A. *Inorg. Chim. Acta* **1998**, *270*, 207. (e) Bazzicalupi, C.; Bencini, A.; Bianchi, A.; Cecchi, M.; Escuder, B.; Fusi, V.; García-España, E.; Giorgi, C.; Luis, S. V.; Maccagni, G.; Marcelino, V.; Paoletti, P.; Valtancoli, B. *J. Am. Chem. Soc.* **1999**, *121*, 6807. (f) Beer, P. D.; Cadman, J.; Lloris, J. M.; Martínez-Máñez, R.; Padilla, M. E.; Pardo, T.; Smith, D. K.; Soto, J. *J. Chem. Soc., Dalton Trans.* **1999**, 127. (g) Anda, C.; Bazzicalupi, C.; Bencini, A.; Berni, E.; Bianchi, A.; Fornasari, P.; Llobet, A.; Giorgi, C.; Paoletti, P.; Valtancoli, B. *Inorg. Chim. Acta* **2003**, *356*, 167.
(7) Mateus, P.; Delgado, R.; Brandão, P.; Carvalho, S.; Félix, V. *Org. Biomol. Chem.* **2009**. DOI: 10.1039/B912940E.
(8) (a) Katayev, E. A.; Boev, N. V.; Myshkovskaya, E.; Khrustalev, V. N.; Ustynyuk, Y. A. *Chem.—Eur. J.* **2008**, *14*, 9065. (b) Katayev, E. A.; Sessler, J. L.; Khrustalev, V. N.; Ustynyuk, Y. A. *J. Org. Chem.* **2007**, *72*, 7244. (c) Moon, K. S.; Singh, N.; Lee, G. W.; Jang, D. O. *Tetrahedron* **2007**, *63*, 9106.
(9) (a) Kwon, T. H.; Jeong, K. *Tetrahedron Lett.* **2006**, *47*, 8539. (b) Kondo, S.; Hiraoka, Y.; Kurumatani, N.; Yano, Y. *Chem. Commun.* **2005**, 1720.
(10) (a) Bisson, A. P.; Lynch, V. M.; Monahan, M.-K. C.; Anslyn, E. V. *Angew. Chem., Int. Ed.* **1997**, *36*, 2340–2342. (b) Niikura, K.; Bisson, A. P.; Anslyn, E. V. *J. Chem. Soc., Perkin Trans. 2* **1999**, 1111–1114.

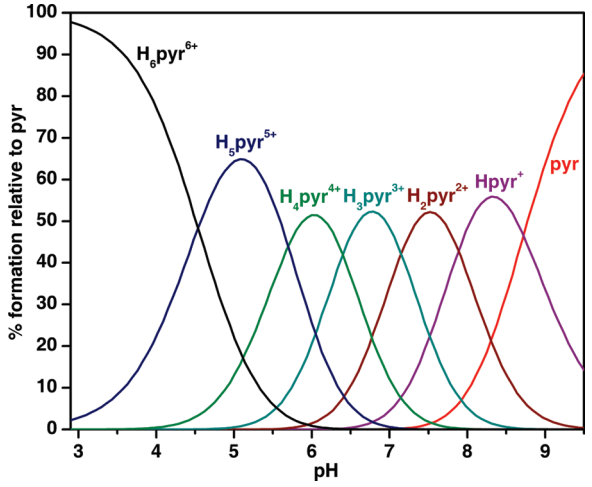

FIGURE 1. Species distribution diagram for the protonation of pyr. $C_{pyr} = 1.0 \times 10^{-3}$ M.

of the receptor due to both increasing electrostatic repulsion between positive charges and to statistical factors. In this pH region there is no protonation of the pyridyl nitrogens, which should be very acidic. The overall basicity of the receptor is lower than expected for secondary amines due to the electron-withdrawing effect of the pyridyl rings and the 2,4,6-triethylbenzene caps. The corresponding distribution curve diagram, represented in Figure 1, shows that the hexaprotonated form, H_6pyr^{6+}, exists as the main species at pH values lower than 4.0.

Binding Studies. The association constants of the protonated forms of pyr, H_npyr^{n+}, with several anions differing in geometry, size, and charge, were determined in MeOH/H_2O (50:50 v/v) solutions at 298.2 K and 0.10 M KTsO. The protonation constants of the anions have been previously determined in the same experimental conditions[7] with the exception of those of arsenate which were found to be 3.01(1), 7.34(1), and 11.33(1). The overall values obtained are collected in Table S1 (Supporting Information) and the stepwise constants are given in Table 2, along with those determined for the related cryptand xyl (see Chart 1) for comparison purposes.

The direct comparison of stepwise constants of both receptors with each anion can lead to erroneous conclusions and to incorrect selectivity attributions, especially when there are overlapping protonation equilibria between receptors and anions. The K_{eff} values, defined as the quotient between the total amount of supramolecular species formed and the total amounts of the free receptor and free substrate at a given pH ($K_{eff} = \sum[H_{i+j}AL]/\sum[H_iA]\sum[H_jL]$, L is the ligand and A the anion),[11] not only allow comparisons between different supramolecular systems studied under the same experimental conditions as it takes into consideration the different basicities of receptors and substrates, but also makes it possible to distinguish the stepwise equilibria that effectively occur from all those that can be established for each case. In Figure 2 the plots of the effective association constant K_{eff} versus pH for the supramolecular associations

(11) Albelda, M. T.; Bernardo, M. A.; Garcia-España, E.; Godino-Salido, M. L.; Luis, S. V.; Melo, M. J.; Pina, F.; Soriano, C. *J. Chem. Soc., Perkin Trans. 2* **1999**, 2545.

TABLE 2. Stepwise Association Constants (log $K_{H_iL_jA_k}$) for the Indicated Equilibria in H_2O/MeOH (50:50 v/v) (T = 298.2 ± 0.1 K and I = 0.10 ± 0.01 M in KTsO)

equilibrium	L = pyr[a]	L = xyl[b]
$H_6L^{6+} + Cl^- \rightleftharpoons [H_6LCl]^{5+}$	2.37(4)	2.01
$H_6L^{6+} + NO_3^- \rightleftharpoons H_6L(NO_3)]^{5+}$	2.54(1)	2.05
$H_6L^{6+} + ClO_4^- \rightleftharpoons [H_6L(ClO_4)]^{5+}$	–[c]	1.79
$H_6L^{6+} + SO_4^{2-} \rightleftharpoons [H_6L(SO_4)]^{4+}$	4.34(1)	5.03
$H_5L^{5+} + SO_4^{2-} \rightleftharpoons [H_5L(SO_4)]^{3+}$	3.23(1)	3.74
$H_4L^{4+} + SO_4^{2-} \rightleftharpoons [H_4L(SO_4)]^{2+}$	2.20(3)	2.69
$H_5L^{5+} + HAcO \rightleftharpoons [H_5L(HAcO)]^{5+}$	1.78(3)	
$H_5L^{5+} + AcO^- \rightleftharpoons [H_5L(AcO)]^{4+}$	2.04(2)	2.28
$H_4L^{4+} + AcO^- \rightleftharpoons [H_4L(AcO)]^{3+}$	2.06(2)	2.20
$H_3L^{3+} + AcO^- \rightleftharpoons [H_3L(AcO)]^{2+}$	1.74(2)	2.27
$H_2L^{2+} + AcO^- \rightleftharpoons [H_2L(AcO)]^{+}$	1.42(6)	2.30
$HL^+ + AcO^- \rightleftharpoons [HL(AcO)]$		2.10
$H_6L^{6+} + H_2PO_4^- \rightleftharpoons [H_6L(H_2PO_4)]^{5+}$	4.05(2)	2.12
$H_5L^{5+} + H_2PO_4^- \rightleftharpoons [H_5L(H_2PO_4)]^{4+}$	3.99(2)	2.98
$H_4L^{4+} + H_2PO_4^- \rightleftharpoons [H_4L(H_2PO_4)]^{3+}$	4.01(2)	2.62
$H_3L^{3+} + H_2PO_4^- \rightleftharpoons [H_3L(H_2PO_4)]^{2+}$	4.00(2)	2.43
$H_2L^{2+} + H_2PO_4^- \rightleftharpoons [H_2L(H_2PO_4)]^{+}$	4.00(2)	
$H_2L^{2+} + HPO_4^{2-} \rightleftharpoons [H_2L(HPO_4)]$	3.68(1)	
$HL^+ + HPO_4^{2-} \rightleftharpoons [HL(HPO_4)]^-$	3.17(1)	
$H_6L^{6+} + H_2AsO_4^- \rightleftharpoons [H_6L(H_2AsO_4)]^{5+}$	3.53(2)	
$H_5L^{5+} + H_2AsO_4^- \rightleftharpoons [H_5L(H_2AsO_4)]^{4+}$	3.58(2)	
$H_4L^{4+} + H_2AsO_4^- \rightleftharpoons [H_4L(H_2AsO_4)]^{3+}$	3.61(2)	
$H_3L^{3+} + H_2AsO_4^- \rightleftharpoons [H_3L(H_2AsO_4)]^{2+}$	3.64(2)	
$H_2L^{2+} + H_2AsO_4^- \rightleftharpoons [H_2L(H_2AsO_4)]^{+}$	3.69(2)	
$H_2L^{2+} + HAsO_4^{2-} \rightleftharpoons [H_2L(HAsO_4)]$	3.37(1)	
$HL^+ + HAsO_4^{2-} \rightleftharpoons [HL(HAsO_4)]^-$	2.89(1)	

[a] Values in parentheses are standard deviations in the last significant figure. [b] The stepwise protonation constants (K_i^H) of xyl are the following: 8.7, 7.86, 7.21, 6.56, 5.96, and 4.99, ref 7. [c] Too small to be determined.

between the protonated forms of pyr and the studied anions, along with those determined for the protonated forms of xyl for comparison, are shown.

Only species of 1:1 receptor to anion stoichiometry were found for the different protonation states of pyr. For fully ionized anions such as chloride, nitrate, and sulfate the association constants increase with increasing positive charge on H_npyr^{n+}, the main interaction being of electrostatic nature. Perchlorate showed virtually no binding to the receptor. Although we have found no differences in the selectivity pattern of H_npyr^{n+} and H_nxyl^{n+} for the series of fully ionized anions ($SO_4^{2-} \gg NO_3^- > Cl^- > ClO_4^-$), the H_npyr^{n+} receptor showed a slightly lower affinity for sulfate and also a lower sulfate to nitrate selectivity. Acetate is weakly bound to both receptors; however, the binding of H_npyr^{n+} with the protonated form of acetate occurs at lower pH.

The most interesting feature of H_npyr^{n+} is that it binds hydrogen phosphate more strongly than does H_nxyl^{n+}, and the effect is more evident at lower pH values. This result can be ascribed to the presence of hydrogen bond acceptors in the cavity, namely the pyridyl nitrogen atoms. Moreover, the association constants for hydrogen phosphate do not vary much in the entire pH region studied. This is due to the fact that hydrogen phosphate and polyammonium receptors can be involved in the formation of several hydrogen bonds in which both the anions and the receptors can act as acceptors or donors.[6e] Hydrogen bonds of the type $-N^+-H\cdots{}^-O-$, $-N^+-H\cdots OH-$, and $-N\cdots HO-$ are expected to be formed at low pH. As deprotonation of the receptor occurs, $-N^+-H\cdots{}^-O-$ hydrogen bonds will become less important while those of type $-N-H\cdots{}^-O-$, $-N-H\cdots OH-$, and $-N\cdots HO-$ are expected to dominate.

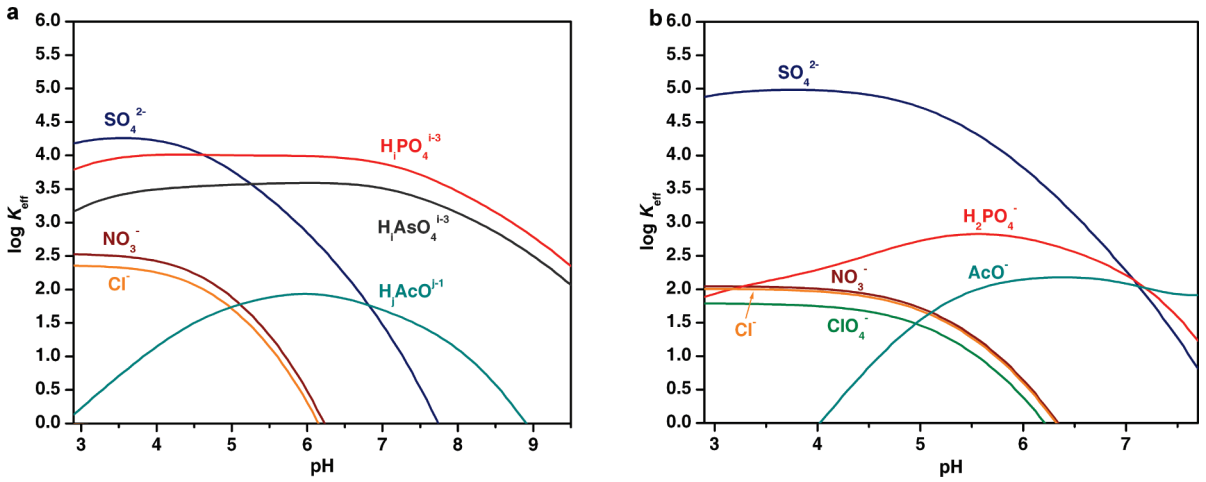

FIGURE 2. Plots of the effective association constant K_{eff} (in log units) versus pH for the supramolecular associations between H_npyr^{n+} (a) and H_nxyl^{n+} (b) and the studied anions. $C_{pyr} = C_{xyl} = C_A = 1.0 \times 10^{-3}$ M.

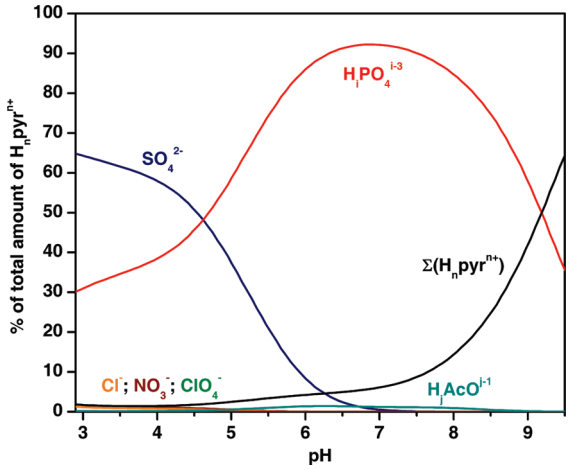

FIGURE 3. Distribution diagram of the overall amounts of supramolecular species formed between the receptor, H_npyr^{n+}, and each anion. Where SO_4^{2-}, $H_iPO_4^{i-3}$, H_jAcO^{j-1}, Cl^-, NO_3^-, and ClO_4^- represent the total amount of the anion bound to the receptor $\sum[H_npyrA]$, A being the indicated anion. $C_{pyr} = C_{anion}/3 = 1 \times 10^{-3}$ M.

Arsenate, being structurally similar to phosphate and having very close protonation constants, presents binding constants slightly lower than phosphate despite having a binding behavior that is completely parallel.

Competitive binding diagrams, in which the overall percentages of the associated species as a function of pH for systems containing the receptor and equimolar amounts of several anions are displayed,[12] give a better overview of the selectivity trends. As shown in Figure 3, at lower pH values the receptor preferably binds sulfate in a mixture of equimolar amounts of chloride, nitrate, perchlorate, dihydrogen phosphate, and acetate, even though it is not selective due to strong competition of dihydrogen phosphate. In fact, it is quite remarkable that dihydrogen phosphate, being less charged that sulfate, is still appreciably bound by the receptor, showing the importance of hydrogen bonding formation. Above pH 4.6 the selectivity is reversed and the receptor preferably binds hydrogen phosphate, due to the fact that it is the only anion that does not rely exclusively on electrostatic interactions and on $-N^+-H\cdots{}^-O-$ hydrogen bonds. At pH 7 the receptor becomes selective for phosphate.

^{31}P NMR Studies. ^{31}P NMR spectra provide a way of getting further insights on the type of hydrogen bonds involved in the binding of phosphate, as the hydrogen bonding interactions in which phosphate acts as hydrogen bond acceptor cause upfield shifts,[13] corresponding to a partial protonation of phosphate, whereas when phosphate acts as a hydrogen bond donor the result is a shift in the opposite direction.

^{31}P NMR spectra of 1:1 H_npyr^{n+} to hydrogen phosphate solutions (H_2O/MeOH 50/50 v/v) were recorded at pH 3.8 and 7.2. Spectra of hydrogen phosphate solutions alone in the same experimental conditions were also recorded for comparison. The results compiled in Figure 4 clearly show that the protonation equilibria of the substrate are disturbed in the presence of H_npyr^{n+}. At pH 3.8, the ^{31}P NMR signal of the 1:1 H_npyr^{n+} to hydrogen phosphate solution shifted upfield relative to the free hydrogen phosphate at the same pH, in agreement with phosphate accepting hydrogen bonds. Under the same conditions, the 1:1 mixture of H_nxyl^{n+} and hydrogen phosphate ^{31}P NMR resonance yields a larger upfield shift than the previous case in spite of its lower K_{eff} value at this pH. This result derives from the fact that H_nxyl^{n+} can act only as a hydrogen bond donor to the substrate, as at this pH the cavity lacks hydrogen bond acceptors, consequently an upfield shift is observed. In the case of H_npyr^{n+} at the same pH value (3.8) both hydrogen bond donors and acceptors are present and the observed chemical shift is an average between the two effects working in opposite ways, in which the hydrogen bond accepting is predominant. In the two cases the broad line width suggests slower receptor−substrate exchanges on the NMR time scale, which is a strong indication of the encapsulation of hydrogen phosphate substrate.

Differently, at pH 7.2 the ^{31}P NMR signal of the 1:1 mixture of H_npyr^{n+} and hydrogen phosphate is shifted

(12) Bianchi, A.; Garcia-España, E. *J. Chem. Educ.* **1999**, *76*, 1727.

(13) (a) Král, V.; Furuta, H.; Shreder, K.; Lynch, V.; Sessler, J. L. *J. Am. Chem. Soc.* **1996**, *118*, 1595. (b) Cozzoner, P. J.; Jardetzky, O. *Biochemistry* **1976**, *15*, 4853.

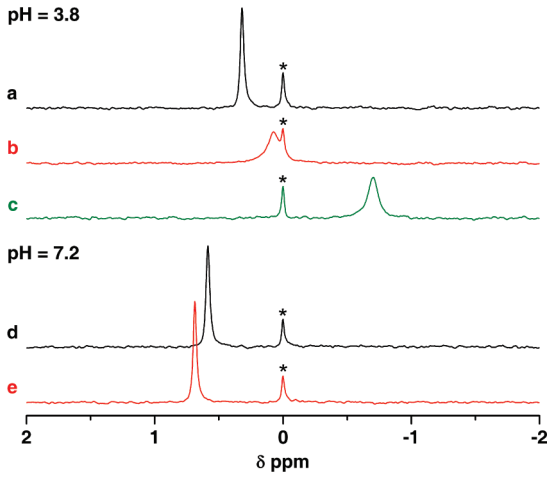

FIGURE 4. ^{31}P NMR spectra of 1:1 H_npyr^{n+}:hydrogen phosphate solutions in H_2O/MeOH at pH 3.8 (b) and 7.2 (e), and for free hydrogen phosphate (a and d) at 298.2 K. For comparison the ^{31}P NMR spectrum of hydrogen phosphate in the presence of 1 equiv of H_nxyl^{n+} (c) is also given in the same experimental conditions. The signal centered at 0 ppm (*) corresponds to H_3PO_4 used as external reference. $C_{pyr} = C_{xyl} = C_{hydrogen\ phosphate} = 8.3 \times 10^{-4}$ M. The pH was adjusted to 3.8 or 7.2 by adding small amounts of HTsO or KOH solutions (see the Experimental Section).

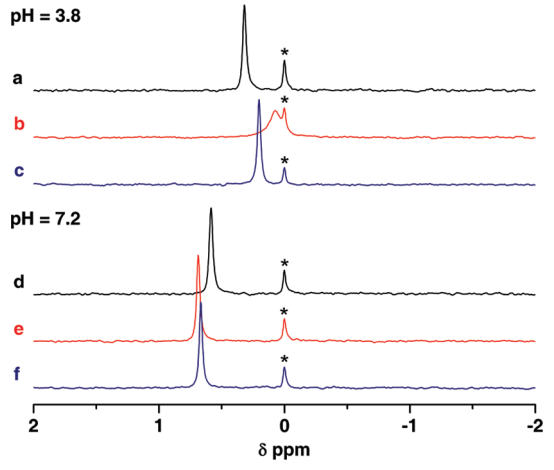

FIGURE 5. ^{31}P NMR spectra of 1:1:1 H_npyr^{n+}:hydrogen phosphate:sulfate solutions in H_2O/MeOH at pH 3.8 (c) and 7.2 (f) at 298.2 K. For comparison, the ^{31}P NMR spectra of 1:1 H_npyr^{n+}: hydrogen phosphate (b and e) and of free hydrogen phosphate (a and d) in the same experimental conditions already shown in Figure 4 were added. The signal centered at 0 ppm (*) corresponds to H_3PO_4 used as external reference. $C_{pyr} = C_{hydrogen\ phosphate} = C_{sulfate} = 8.3 \times 10^{-4}$ M. The pH was adjusted to 3.8 or 7.2 by adding small amounts of HTsO or KOH solutions (see the Experimental Section).

downfield relative to the free hydrogen phosphate, indicating that the hydrogen bond donating from hydrogen phosphate to the receptor is predominant, in agreement with the partial deprotonation of the receptor at this pH with the concomitant −N···HO− hydrogen bonds significance.

A competitive experiment also followed by ^{31}P NMR was performed in which to the 1:1 mixture of H_npyr^{n+} and hydrogen phosphate 1 equiv of sulfate was added. The spectra shown in Figure 5 revealed that at pH 3.8 sulfate displaces hydrogen phosphate from the receptor, although not completely, while at pH 7.2 the presence of sulfate has almost no influence on the binding of hydrogen phosphate. These results are in excellent agreement with those determined by potentiometry and expressed in Figure 3.

Crystallographic Studies. Single crystal structures of anion associations of H_6pyr^{6+} receptor with nitrate, sulfate, and phosphate were determined by X-ray diffraction and they are consistent with the existence of $[(H_6pyr)(NO_3)_3(H_2O)_3]^{3+}$, $[(H_6pyr)(SO_4)_2(H_2O)_4]^{2+}$, and $[(H_6pyr)(HPO_4)_2(H_2PO_4)(H_2O)_2]^{+}$ cations.

The asymmetric unit of the nitrate association is composed of one hexaprotonated H_6pyr^{6+} receptor, six nitrate anions, and seven water molecules, which is consistent with molecular formula $[(H_6pyr)(NO_3)_3(H_2O)_3](NO_3)_3\cdot 4H_2O$. The structure of $[(H_6pyr)(NO_3)_3(H_2O)_3]^{3+}$ association, presented in Figure 6, shows one nitrate anion inserted into the macrobicyclic cage adopting an almost parallel disposition to the 2,4,6-triethylbenzene caps. The nitrate is located at 3.31 and 3.22 Å from these two aromatic rings, suggesting that the encapsulated anion is stabilized by $\pi-\pi$ interactions. This nitrate anion is also involved in a network of hydrogen bonds with four bridging water molecules and NH_2 binding groups, as shown in Figure 6b,c. The nitrate is 1.25 Å deviated from the N_6 center binding cage establishing only three straight N−H···O hydrogen bonds with two N−H neighbor binding sites at H···O distances of 2.22, 2.30, and 2.38 Å, drawn as green dashed lines in Figure 6b,c. Each bridging water molecule is hydrogen bonded to the included nitrate oxygen and two N−H binding sites from adjacent NH_2 binding groups leading to O···O distances of 2.767(7), 2.797(6), and 2.823(7) Å, respectively, and O···N distances between 2.816(7) and 3.002(7) Å. Two water molecules are also stabilized by further hydrogen bonds formed with two nitrate anions, located at the periphery of the cage, at O···O distances of 2.895(7) and 2.874(7) Å. These two nitrate anions interact with receptor NH_2 binding sites with N···O distances ranging between 2.9717(7) and 3.041(7) Å. The dimensions of all N−H···O bonds in $[(H_6pyr)(NO_3)_3(H_2O)_3](NO_3)_3\cdot 4H_2O$ are given in Table S3 (Supporting Information). The analysis of hydrogen bonds is consistent with the existence of a $\{(NO_3)_3(H_2O)_3\}^{3-}$ cluster with a nitrate embedded into the cage and stabilized by means of multiple hydrogen bonds and electrostatic interactions formed with the highly charged H_6pyr^{6+} receptor.

In the case of the sulfate association, the asymmetric unit is composed of ten crystallization water molecules, four sulfate anions, and one H_6pyr^{6+} cation. The charge balance of the asymmetric unit content requires necessarily the existence of two protons, which can be accommodated by one H_2SO_4 neutral species or more likely by two hydrogen sulfate anions (HSO_4^-). The main structural features of sulfate association are presented in Figure 7. Although the atomic positions of some water hydrogen atoms were discernible from the last difference Fourier maps, these two extra protons were not. However, their location can be inferred from the S−O distances pattern. Indeed, two sulfate anions display one S−O distance of 1.560(2) and 1.566(2) Å longer than the remaining ones ranging between 1.462(2) and 1.439(2) Å. By contrast in the other two sulfate counterions, all four S−O distances are equivalent varying only from 1.472(2) to 1.494(2) Å. This structural feature suggests that the two protons are bonded to oxygen atoms of two sulfate anions

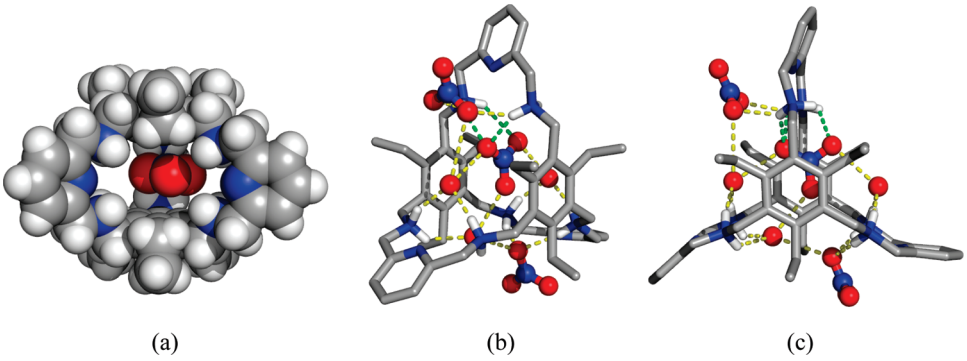

FIGURE 6. Perspective views illustrating different structural features of the association between nitrate and the H_6pyr^{6+} receptor: (a) Space-filling model showing the nitrate anion inserted into the macrobicyclic cavity and its relative position toward to the two 2,4,6-triethylbenzene rings; (b and c) views emphasizing the N−H···O hydrogen bonding network and the receptor conformation adopted. The color scheme used is carbon in gray, nitrogen in blue, hydrogen in white, and oxygen atoms in red. N−H···O hydrogen bonds are drawn as yellow and green dashed lines and the C−H hydrogen atoms have been omitted for clarity.

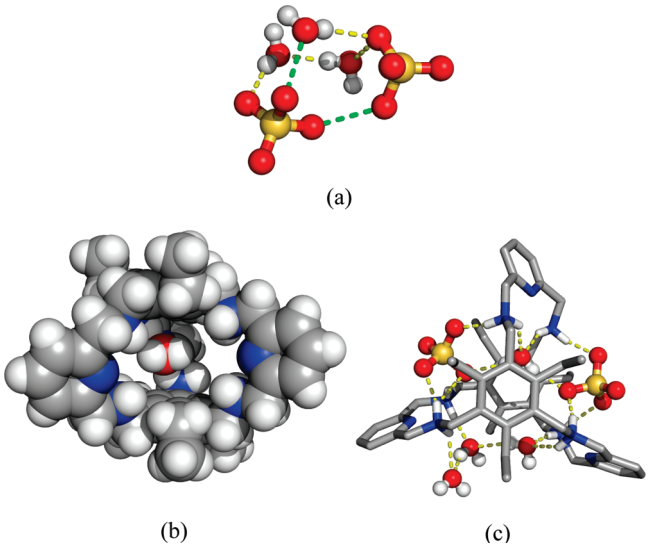

FIGURE 7. Three views illustrating different structural features of the association of sulfate with H_6pyr^{6+} receptor: (a) view of the $\{(HSO_4)_2(H_2O)_3\}^{2-}$ hydrogen bonded cluster with yellow dashed lines showing the potential location of HSO_4^- protons; (b) space-filling model showing one crystallization water molecule inserted into the macrobicyclic cavity; (c) view showing the receptor conformation and N−H···O hydrogen bond network formed between sulfate anions, water molecules, and 12 receptor N−H binding sites. The remaining details are given in Figure 6.

with S−O longer distances. Furthermore, the crystal packing diagram shows that these two anions are hydrogen bonded by three water molecules and by the two protons with one S=O—H···O=S distance of 2.632(3) Å and one S=O—H···OH_2 distance of 2.559(3) Å, green dashed lines in Figure 7a. Furthermore, the two HSO_4^- anions do not interact directly with the receptor, while the two SO_4^{2-} anions are assembled together with four water molecules as shown in Figure 7b,c. This associated entity contains a water molecule hydrogen bonded to two sulfate anions with H···O distances of 2.01 and 2.03 Å as well as a trimer of water molecules with H···O distances of 1.99 and 2.17 Å. The $\{(SO_4)_2(H_2O)\}^{4-}$ and $\{(H_2O)\}_3$ entities are stabilized through multiple and cooperative N−H···O hydrogen bonds with the receptor, as shown in Figure 7c. The dimensions of all N−H···O and O−H···O hydrogen bonding interactions found in $[(H_6pyr)(SO_4)_2(H_2O)_4](HSO_4)_2\cdot 6H_2O$ are given in Table S4 (Supporting Information). The water molecule that bridges both sulfate anions, see Figure 7b, is completely encapsulated into the macrobicyclic cage and hydrogen bonded to two N−H binding sites from adjacent amino−alkyl linkages with N···O distances of 2.849(2) and 2.945(2) Å. The two sulfate anions interact with H_6pyr^{6+} through three N−H···O hydrogen bonds with N···O distances between 2.773(2) and 2.872(2) Å. This binding arrangement contrasts with that of $\{(SO_4)(H_2O)_6\}^{2-}$ in $[(H_6xyl)(SO_4)(H_2O)_6]^{4+}$ (see Chart 1),[7] where the sulfate anion is entirely embedded inside of the macrocyclic cage.

In the phosphate assembled molecule the asymmetric unit is composed of one H_6pyr^{6+} cation, four phosphate anions, and eighteen water molecules. The most relevant structural features of phosphate association are illustrated in Figure 8. The charge balance of the molecular formula is consistent with the existence of two $H_2PO_4^-$ and two HPO_4^{2-} independent anions, taking into account the conditions used to grow the crystals. These protons were not revealed by single-crystal X-ray determination, and similarly to what was done for the sulfate association, the protons to the phosphate species were tentatively assigned from P−O distances. Two phosphate anions exhibit one P−O distance of 1.582(3) and 1.581(3) Å, respectively, which are slightly larger than the remaining three distances ranging from 1.540(3) and 1.513(3) Å. This suggests that these two anions are the HPO_4^{2-}. The third phosphate, which is not directly involved in hydrogen bonds with H_6pyr^{6+}, contains two P−O distances of 1.579(3) and 1.583(3) Å longer than the remaining two 1.496(4) and 1.501(3) Å, which seems to indicate that this species is $H_2PO_4^-$. Finally, taking into account this analysis, the forth counteranion is necessarily $H_2PO_4^-$, and has P−O distances varying between 1.496(3) and 1.547(4) Å, which are apparently not consistent with such species. Two water molecules, three phosphate anions (two HPO_4^{2-} and eventually one $H_2PO_4^-$), and H_6pyr^{6+} are assembled in the $[(H_6pyr)(HPO_4)_2(H_2PO_4)(H_2O)_2]^+$ cation, shown in Figure 8. Two water molecules, separated by an O···O distance of 2.945(4) Å, are hydrogen bonded and located inside of the cage, see Figure 8a. Both water molecules are linked to one phosphate oxygen acceptor with O···O distances of 2.623(4) and 2.620(4) Å and two N−H binding sites from adjacent amino−alkyl linkages with N···O distances of 2.866(4),

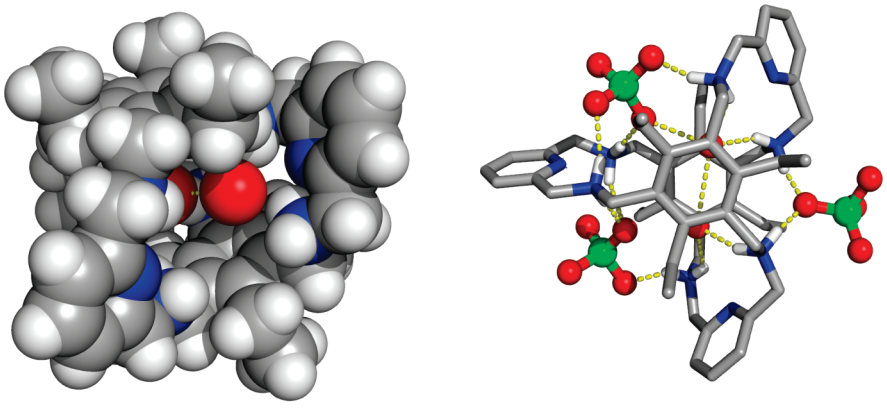

FIGURE 8. Two views illustrating different structural features of the association between phosphate and H_6pyr^{6+} receptor: (a) space-filling model showing two crystallization water molecules inserted into the macrobicyclic cavity; (b) view showing the receptor conformation and the N−H···O hydrogen bonding interactions formed. The remaining details are given in Figure 6.

2.999(4), 2.873(5), and 2.973(4) Å. The three anions surround the macrobicycle: two of them (HPO_4^{2-} species) are linked by three short N−H···O bonding interactions to N−H binding sites while the third one ($H_2PO_4^-$) establishes only two N−H···O hydrogen bonds. The dimensions of all hydrogen bonds found in $[(H_6pyr)(HPO_4)_2(H_2PO_4)(H_2O)_2](H_2PO_4)\cdot 16H_2O$ are also listed in Table S5 (Supporting Information).

The comparison of the structures of the three associations provides further information on the possible conformations of the receptor. In fact, the H_6pyr^{6+} receptor in $[(H_6pyr)(NO_3)_3(H_2O)_3]^{3+}$ displays nearly a C_3 symmetry with 3-fold axis perpendicular to parallel 2,4,6-triethylbenzene caps as apparent from Figure 6b, which shows a view of the nitrate supermolecule along these aromatic rings. Indeed, the lines determined by the centroids of pyridine spacers and mass center of the cage make angles (α angles) of 114.0°, 122.8°, and 123.3°. The interplanar distance between the two caps (β distance) is 6.543 Å. In the sulfate association the α angles are 113.2° , 121.2°, and 125.2° and the β distance is 6.939 Å, but the molecular diagram presented in Figure 7c indicates an evident absence of C_3 symmetry motivated by the spatial disposition of pyridine rings and staggered arrangement of 2,4,6-triethylbenzene substituents. A comparable macrobicyclic conformation was observed for the association with phosphate, Figure 8b, but the α angles 103.6°, 115.5°, and 140.0° are more deviated from the ideal value of 120° and the β distance of 7.353 Å is longer. Equivalent conformations were found in the crystal structures of associations of related benzene-capped hexaprotonated cryptands with halide[14] and sulfate[7] anions. However, in all cases the reported distances between the two parallel benzene caps are much longer ca. 9 Å. For example, in the $[(H_6xyl)(SO_4)(H_2O)_6]^{4+}$ crystal structure,[7] the β distance is 9.157 Å and α angles range from 117.7° to 120.6°. This comparison indicates that this cryptand receptor type has apparent rigid structures, but with enough flexibility to trap water molecules assembled or not with anions in their cages. In particular, in the three anion supramolecular associations reported here, the H_6pyr^{6+} conformation is determined by the N−H···O hydrogen bonding interactions established with anions as counterions located in the cryptand cavity periphery, rather than by the mismatch of sizes between the cage and the encapsulated substrate.

(14) Arunachalam, M.; Ravikumar, I.; Ghosh, P. *J. Org. Chem.* **2008**, *73*, 9144.

Conclusions

Solution studies revealed that the H_npyr^{n+} receptor is able to discriminate dinegative sulfate from mononegative anions NO_3^-, Cl^-, and ClO_4^-, the main interaction being of electrostatic nature, as the association constants increase with increasing positive charges on H_npyr^{n+}. This means that the association is only governed by the charge and hydrogen bond donating ability of the receptor, and in this sense H_npyr^{n+} has a behavior similar to that of H_nxyl^{n+}.[7] However, the present work also shows how the selectivity pattern can be modulated by slight changes in the framework of the receptor. In fact, the change of the *m*-xylyl spacers of H_nxyl^{n+} to pyridyl ones in H_npyr^{n+} led to remarkable differences on the association behavior of the receptor with anions. Apparently, as in phosphate binding protein (PBP), the presence of hydrogen bond acceptors in the H_npyr^{n+} receptor enhances the affinity for hydrogen phosphate. Therefore, at low pH the H_npyr^{n+} receptor has an affinity for dihydrogen phosphate of the order of sulfate, in spite of the lower charge of the former anion, and it is capable of effectively competing with sulfate at higher pH, being selective for hydrogen phosphate at pH about 7.0. Furthermore, the fact that the receptor shows such a marked preference for hydrogen phosphate based mainly in its hydrogen bond accepting/donating ability in a highly competitive media such as water/methanol mixed solvent is quite remarkable.

The crystallographic studies reported here are apparently in contradiction with the solution studies, namely, sulfate and phosphate anions located outside of the cavity and no evidence of the −N···HO− hydrogen bonds formation, which are important features in light of the solution studies. However, "considering the crystal structure as the unique in solution is a broad simplification of a complex process, where only a collection of individual arrangements represents the structural ensemble, even when the configuration of

the assembled molecule observed in the crystal is the most stable one in solution".[15] Thus the crystal structures should best be viewed as snapshots of the binding event. Despite this, the reported crystal structures provided important information on the different possible conformations of the receptor.

The present study allowed us to conclude that, although H_npyr^{n+} is not as efficient in discriminating hydrogen phosphate from sulfate as the PBP, it is to the best of our knowledge the artificial polyamine compound with highest reported phosphate/sulfate selectivity in aqueous solutions at pH about 7.0[6a−c,e,g,16,17] (see Figure S7 in the Supporting Information).

Experimental Section

Synthesis. Schiff Base of pyr. A solution of 1,3,5-tris(aminomethyl)-2,4,6-triethylbenzene (300 mg, 1.2 mmol) in MeCN (30 cm^3) was added dropwise over 7 min to a magnetically stirred solution of 2,6-pyridinedicarbaldehyde (244 mg, 1.8 mmol) dissolved in MeCN (30 cm^3) and the mixture was left under stirring overnight. A white precipitate formed, which was separated by filtration and washed with MeCN (about 100 cm^3) to remove any unreacted starting materials. The precipitate was suspended in $CHCl_3$ (100 cm^3), ultrasonicated for 1 h, and filtered. Evaporation of the solvent yielded the desired hexaimine, which was dried in vacuum.Yield 60%; ^{1}H NMR (400 MHz, $CDCl_3$, 298.2 K, TMS) δ 8.07 (d, J = 8.0 Hz, 6 H, H3, H5, py), 7.91 (s, 6 H, HC═N), 7.70 (t, J = 7.6 Hz, 3H, H4, py), 5.07 (s, 12 H, CH_2Ph), 2.22 (q, J = 8.0 Hz, 12 H, PhCH_2CH$_3$), 1.18 (t, J = 8.0 Hz, 18H, PhCH$_2$CH_3) ppm; ^{13}C NMR (100 MHz, $CDCl_3$, 298.2 K, TMS) δ 159.5 (C═N), 154.8 (C2, C6, py), 144.3 (C1, C3, C5, Ph), 136.7 (C4, py), 131.1 (C2, C3, C4, Ph), 121.8 (C3, C5, py), 54.4 (CH_2Ph), 23.8 (PhCH_2CH$_3$), 16.0 (PhCH$_2$CH_3) ppm.

pyr. Solid $NaBH_4$ (1.226 g, 32.4 mmol) was added in small portions to a magnetically stirred suspension of the hexaimine (428 mg, 0.54 mmol) in MeOH (65 cm^3). The mixture was stirred at rt for 2 h, and under reflux overnight. Then the solution was evaporated under vacuum to almost dryness, H_2O (20 cm^3) was added, and the methanol was evaporated. The solution was made strongly basic with 6 M KOH and extracted with $CHCl_3$ (3 × 50 cm^3). The organic portions were collected, dried over anhydrous sodium sulfate, filtered, evaporated to dryness, and dried under vacuum. Yield 90%; mp 110 °C dec; ^{1}H NMR (400 MHz, $CDCl_3$, 298.2 K, TMS) δ 7.46 (t, J = 8.0 Hz, 3 H, H4, py), 6.99 (d, J = 8.0 Hz, 6 H, H3, H5, py), 3.85 (s, 12 H, pyCH_2), 3.71 (s, 12 H, CH_2Ph), 2.70 (q, J = 8.0 Hz, 12 H, PhCH_2CH$_3$), 1.03 (t, J = 8.0 Hz, 18 H, PhCH$_2$CH_3) ppm; ^{13}C NMR (100 MHz, $CDCl_3$, 298.2 K, TMS) δ 157.6 (C2, C6, py) 141.7 (C1, C3, C5, Ph), 135.5 (C4, py), 132.6 (C2, C3, C4, Ph), 119.5 (C3, C5, py), 54.5 (pyCH_2), 46.6 (CH_2Ph), 21.6 (PhCH_2CH$_3$), 15.7 ppm (PhCH$_2$CH_3); ESI-MS (MeOH) m/z (%) 808.6 $[M + H]^+$. Anal. Calcd for $C_{51}H_{69}N_9 \cdot 0.5CHCl_3 \cdot 2.5H_2O$: C 67.76, H 8.23, N 13.81. Found: C 67.93, H 8.34, N 13.71.

Crystals of $[(H_6pyr)(NO_3)_3(H_2O)_3](NO_3)_3 \cdot 4H_2O$. The pyr compound (4.04 mg, 5 μmol) was dissolved in acetone (500 μL) and 65% HNO_3 (2.077 μL) was added. Immediately a white precipitate was formed. Water (90 μL) was added and the solution was heated until it was clear, then the mixture was allowed to slowly cool to rt. Single colorless crystals suitable for X-ray crystallography were grown overnight.

Crystals of $[(H_6pyr)(SO_4)_2(H_2O)_4](HSO_4)_2 \cdot 6H_2O$. The pyr compound (4.04 mg, 5 μmol) was dissolved in acetone (500 μL) and 97% H_2SO_4 (1.658 μL) was added. Water (90 μL) was added and the solution was treated as in the latter case. Single colorless crystals suitable for X-ray crystallography were grown overnight.

Crystals of $[(H_6pyr)(HPO_4)_2(H_2PO_4)(H_2O)_2](H_2PO_4) \cdot 16H_2O$. The pyr compound (4.04 mg, 5 μmol) was dissolved in acetone (500 μL) and 85% H_3PO_4 (2.053 μL) was added. Water (60 μL) was added to the white precipitate formed, and the solution was treated as before. Single colorless crystals suitable for X-ray crystallography were grown overnight.

Potentiometric Measurements. Reagents and Solutions. All solutions were prepared in water/methanol (50:50 v/v) solvent. A stock solution of the receptor was prepared at ca. 1.5×10^{-3} M. Anion solutions were prepared at 0.1 M from the corresponding potassium salts and the concentrations were checked by titration with standard 0.100 M KOH solutions. Carbonate-free solutions of the KOH titrant were prepared as described earlier.[7] These solutions were discarded every time carbonate concentration was about 0.5% of the total amount of base. The titrant solutions were standardized (tested by Gran's method).[18]

Equipment and Working Conditions. The equipment used was described before.[7] The ionic strength of the experimental solutions was kept at 0.10 ± 0.01 M with KTsO, and temperature was maintained at 298.2 ± 0.1 K. Atmospheric CO_2 was excluded from the titration cell during experiments by passing purified nitrogen across the top of the experimental solution. The glass electrode was pretreated by soaking it in the water−methanol (50:50 v/v) solution over a period of 2 days, in order to prevent erratic responses.

Measurements. The $[H^+]$ of the solutions was determined by the measurement of the electromotive force of the cell, $E = E'^\circ + Q \log[H^+] + E_j$. The term pH is defined as $-\log [H^+]$. E'°, Q, E_j, and K'_w were determined by titration of a solution of known hydrogen ion concentration at the same ionic strength, using the acid pH range of the titration. The liquid-junction potential, E_j, was found to be negligible under the experimental conditions used. The value of K'_w was determined from data obtained in the alkaline range of the titration, considering E'° and Q valid for the entire pH range, and found to be equal to $10^{-13.91}$ in our experimental conditions. Before and after each set of titrations the glass electrode was calibrated by titration of 1.0×10^{-3} M standard HCl solution with standard KOH. The potentiometric equilibrium measurements were carried out with 20.00 cm^3 of ~1.56×10^{-3} M pyr solution diluted to a final volume of 30.00 cm^3, in the absence of anions, then in the presence of each anion at 1:3 R:A ratios (R = receptor and A = anion). In each titration 85 to 120 points were collected, and a minimum of two titration curves were performed. Care has been taken to maintain unaltered the methanol−water ratio in measured solution. The exact concentration of pyr was obtained by determination of the excess of acid present in a mixture of pyr and standard *p*-toluenesulfonic acid (1.0×10^{-2} M) by titration with standard KOH solution.

Calculation of Equilibrium Constants. Overall protonation constants, β_i^H, of both ligand and anions in the same experimental conditions were calculated by fitting the potentiometric data obtained for all the performed titrations with the HYPERQUAD program.[19] All these constants were taken as fixed values to obtain the equilibrium constants of the new species from the experimental data corresponding to all titrations at 1:3 R:A ratio, using also the HYPERQUAD program. The initial computations were obtained in the form of overall stability constants, $\beta_{H_hL_lA_a}$ values, $\beta_{H_hL_lA_a} = [H_hL_lA_a]/[H]^h[L]^l[A]^a$. The

(15) Schmidtchen, F. P. *Coord. Chem. Rev.* **2006**, *250*, 2918.
(16) Motekaitis, R. J.; Utley, W. B.; Martell, A. E. *Inorg. Chim. Acta* **1993**, *21*, 15.
(17) Arranz, P.; Bencini, A.; Bianchi, A.; Diaz, P.; García-España, E.; Giorgi, C.; Luis, S. V.; Querol, M.; Valtancoli, B. *J. Chem. Soc., Perkin Trans. 2* **2001**, 1765.
(18) Rossotti, F. J.; Rossotti, H. J. *J. Chem. Educ.* **1965**, *42*, 375.
(19) Gans, P.; Sabatini, A.; Vacca, A. *Talanta* **1996**, *43*, 1739.

errors quoted are the standard deviations of the overall association constants given directly by the program for the input data, which include all the experimental points of all titration curves. Distribution diagrams were plotted from the calculated constants with the HYSS program.[20] The species considered in a particular model were those that could be justified by the principles of supramolecular chemistry.

^{31}P NMR Studies. Solutions of the hydrogen phosphate associations with $(H_6pyr)(TsO)_6$ and $(H_6xyl)(TsO)_6$ were prepared in H_2O/MeOH 50:50 v/v at 8.30×10^{-4} M (1:1 receptor to anion ratio). The pH was adjusted to 3.8 or 7.2 by adding small amounts of HTsO or KOH solutions. Hydrogen phosphate solutions in the absence of receptors were also prepared at the same concentration and at the same pH values.

Competition experiments were carried out by mixing equimolar amounts of potassium dihydrogen phosphate, potassium sulfate, and $(H_6pyr)(TsO)_6$ (8.30×10^{-4} M) in H_2O/MeOH 50:50 v/v and the pH was adjusted to 3.8 or 7.2 by adding small amounts of HTsO or KOH solutions.

In all cases an internal capillary tube containing D_2O and H_3PO_4 was used for locking and referencing purposes during spectra acquisition.

Crystallography. The single-crystal X-ray data of the anion binding complexes were collected on a CCD Bruker APEX II at 150(2) K using graphite monochromatized Mo Kα radiation ($\lambda = 0.71073$ Å). The pertinent crystallographic data are given in Table S2 (Supporting Information). Data reduction including a multiscan absorption correction was carried out with the SAINT-NT from Bruker AXS. The structures were solved by direct methods and by subsequent difference Fourier syntheses and refined by full-matrix least-squares on F^2, using the SHELX-97 suite.[21] Anisotropic thermal parameters were used for all non-hydrogen atoms. One nitrate counterion of $[(H_6pyr)(NO_3)_3(H_2O)_3](NO_3)_3 \cdot 4H_2O$ displays high thermal displacements, which were ascertained to thermal disorder. The N−H and C−H hydrogen atoms were introduced in the structure refinement at calculated positions. The hydrogen atomic positions of water molecules were obtained from the last Fourier difference maps for sulfate association while for phosphate and nitrate anion association they were not found and therefore they were not included in the structure refinement. The protons required by the charge balance of the molecular formulas of sulfate and phosphate associations were not taken into account. All hydrogen atoms were refined $U_{iso} = 1.2U_{eq}$ of the parent atom. Molecular diagrams were drawn with PyMOL.[22]

Acknowledgment. The authors acknowledge FCT, with coparticipation of the European Community funds FEDER, for financial support under projects PTDC/QUI/56569/2004 and PTDC/QUI/68582/2006. The NMR spectrometers are part of the National NMR Network and were acquired with funds from FCT and FEDER. We also acknowledge M. C. Almeida for providing elemental analysis and ESI-MS data from the Elemental Analysis and Mass Spectrometry Service at the ITQB. Pedro Mateus thanks FCT for grant SFRH/BD/36159/2007.

Supporting Information Available: NMR (^{1}H, ^{13}C, COSY, NOESY, and HMQC) and ESI-mass spectra of the pyr reported compound, table with the overall association constants (log $\beta_{H_hL_lA_a}$), plot of phosphate/sulfate selectivity profile as a function of pH for H_npyr^{n+} and related polyamine compounds, and tables of hydrogen bond dimensions of the crystal structures of nitrate, sulfate and phosphate associations. This material is available free of charge via the Internet at http://pubs.acs.org.

(20) Alderighi, L.; Gans, P.; Ienco, A.; Peters, D.; Sabatini, A.; Vacca, A. *Coord. Chem. Rev*. **1999**, *184*, 311.

(21) Sheldrick, M. *Shelx-97, Program for the Solution of Crystal Structures*; University of Göttingen: Göttingen, Germany, 1997.

(22) DeLano, W. L. *The PyMOL Molecular Graphics System DeLano Scientific*, San Carlos, CA, 2002. http://www.pymol.org.